HHS Public Access

Author manuscript

Exp Eye Res. Author manuscript; available in PMC 2022 December 01.

Published in final edited form as:

Exp Eye Res. 2021 December ; 213: 108838. doi:10.1016/j.exer.2021.108838.

Assessment of Retinal Oxygen Metabolism, Visual Function, Thickness and Degeneration Markers after Variable Ischemia/ Reperfusion in Rats

Nathanael Matei[1], **Sophie Leahy**[1], **Norman P. Blair**[2], **Mahnaz Shahidi**[1]

[1]Department of Ophthalmology, University of Southern California, Los Angeles, California, United States

[2]Department of Ophthalmology and Visual Sciences, University of Illinois at Chicago, Chicago, Illinois, United States

Abstract

After total retinal ischemia induced experimentally by ophthalmic vessel occlusion followed by reperfusion, studies have reported alterations in retinal oxygen metabolism (MO_2), delivery (DO_2), and extraction fraction (OEF), as well as visual dysfunction and cell loss. In the current study, under variable durations of ischemia/reperfusion, changes in these oxygen metrics, visual function, retinal thickness, and degeneration markers (gliosis and apoptosis) were assessed and related. Additionally, the prognostic value of MO_2 for predicting visual function and retinal thickness outcomes was reported. Sixty-one rats were divided into 5 groups of ischemia duration (0 [sham], 60, 90, 120, or 180 minutes) and 2 reperfusion durations (1 hour, 7 days). Phosphorescence lifetime and blood flow imaging, electroretinography, and optical coherence tomography were performed. MO_2 reduction was related to visual dysfunction, retinal thinning, increased gliosis and apoptosis after 7-days reperfusion. Impairment in MO_2 after 1-hour reperfusion predicted visual function and retinal thickness outcomes after 7-days reperfusion. Since MO_2 can be measured in humans, findings from analogous studies may find value in the clinical setting.

Keywords

ophthalmic vessel occlusion; retinal ischemia; retinal oxygen metabolism

Correspondence should be addressed to Dr. Mahnaz Shahidi, Department of Ophthalmology, University of Southern California, 1450 San Pablo St, Los Angeles, CA 90033. mshahidi@usc.edu.

Author contributions

The idea and experimental design of the present study were made by Mahnaz Shahidi and Norman P. Blair. Sophie Leahy performed imaging and image analysis, and Nathanael Matei performed biochemical evaluations. The manuscript was drafted by Nathanael Matei, and critical revisions of the manuscript were made by all authors.

Disclosure

MS holds a patent for the oxygen imaging technology. The authors have no conflict of interest.

INTRODUCTION

Ischemia is defined as inadequate blood flow to tissues and organs, and if their metabolic demands cannot be sustained by exposure to both oxygen and glucose, ischemic injury occurs (Stitt et al., 2011). The incidence of ischemia-related pathologies such as myocardial infarction, angina pectoris, stroke and retinopathies have been on the rise in the general population (Stitt et al., 2011). Specifically, retinal ischemia is associated with retinal vascular occlusions, carotid occlusive disorders, diabetic retinopathy, and glaucoma, leading causes of visual impairment and blindness (D'Onofrio and Koeberle, 2013; Osborne et al., 2004).

The ophthalmic vessel occlusion (OVO) animal model aims to mimic the clinical, pathological sequelae of retinal ischemia. Although there are limitations in using animal models due to variations in retinal vascular patterns and function across species, the retinal and cerebral vascular structure in pigs (Moren et al., 2009; Pournaras, 1995), non-human primates (Bhisitkul et al., 2005; Hayreh et al., 1980), and rats (Shabanzadeh et al., 2018; Yamori et al., 1976) closely resembles that of humans. In the OVO model, ischemic durations greater than 60 minutes have resulted in reductions in retinal oxygen metabolism (MO_2) and delivery (DO_2), increased oxygen extraction fraction (OEF) (20-minute reperfusion) (Blair et al., 2019), electrophysiological dysfunction (2- to 21-day reperfusion) (Schmid et al., 2014; Sun et al., 2013; Zhang et al., 2008), and histological damage (1- to 28-day reperfusion) (Dominguez et al., 2015; Ebneter et al., 2017; Genevois et al., 2004). However, there is no information on MO_2, DO_2, and OEF under variable ischemia and reperfusion durations.

The severity of retinal ischemic injury depends on the duration and level of impaired blood flow, such that tissue damage increases as ischemia duration and impairment level increase (Fry et al., 2018; Hayreh, 2001; Leske et al., 2007; Moore et al., 2008). Under ischemic conditions, due to a deficiency in oxygen supply, MO_2 is reduced, that is, energy production becomes impaired. Accordingly, assessment of MO_2 in relation to visual, anatomical and biochemical outcomes appears to be promising to characterize the state of retinal tissue following ischemic injury. However, limited information is available on the effect of ischemia and reperfusion on MO_2.

The brain and retina are parts of the central nervous system. Therefore, knowledge of ischemic brain injury can point the way to better understand pathophysiology of retinal ischemia. Thus far, reperfusion remains the most efficacious intervention in cerebral ischemic related pathologies, but due to a limited and dynamic window of opportunity, it may exacerbate the adverse outcomes associated with ischemia-- a phenomenon termed ischemia-reperfusion injury (Wu et al., 2018). To date, in acute ischemic stroke patients, one of the most metabolically precise ways to calculate and distinguish viable tissue that is at-risk of cell-death is through positron emission tomography (PET), where at-risk tissue has an increased rate of oxygen extraction compared to normal tissue (Aanerud et al., 2012). Using the sensitivity of PET, cerebral metabolic rate of oxygen consumption, similar to retinal MO_2, has been shown to accurately detect salvageable tissue to exist beyond conventional acute settings (<24 hours) (Verro and Chow, 2009) as well as predict cellular

survival (Touzani et al., 1997). In another prospective imaging study, the cerebral metabolic rate of oxygen was highly predictive of both cell death and reperfusion-dependent survival of tissue at risk for cell death (An et al., 2015). Given the predictive power of cerebral metabolic rate of oxygen consumption following ischemic injury, findings on retinal MO_2 following retinal ischemia/reperfusion may also display a prognostic value.

There remains an unmet need for detecting salvageable tissue in the acute setting of retinal ischemia as well as predicting outcomes after injury. Knowledge of MO_2 may help identify a window of opportunity for reversing tissue damage and examining the efficacy of reperfusion after variable durations of ischemia. In the present study, we tested two hypotheses: 1) MO_2 reduction is related to visual dysfunction, retinal thinning, increased degeneration markers (gliosis and apoptosis) after ischemia followed by 7 days of reperfusion, and 2) MO_2 impairment shortly after ischemia/reperfusion injury can predict impairments in visual function and retinal thickness outcomes after 7 days of reperfusion.

MATERIALS AND METHODS

Animals

All experiments were approved by the University of Southern California Institutional Animal Care and Use Committee, complied with the guidelines of the statement of Use of Animals in Ophthalmic and Vision research by the Association for Research in Vision and Ophthalmology, and reported according to the Animal Research: Reporting of In Vivo Experiment guidelines. Sixty-one Long-Evans rats were studied (age: 13.5±2.4 weeks; weight: 412±47 g). Animals were divided into 5 ischemic duration groups (0 [sham], 60, 90, 120, 180 minutes) and 2 reperfusion durations (1 hour, 7 days). Vascular oxygen tension and blood flow imaging were performed after 1 hour or 7 days of reperfusion. Electroretinography (ERG) and spectral-domain optical coherence tomography (OCT) were performed coupled with ex vivo biochemical evaluations after 7 days of reperfusion. The experimental outline and the number of animals in each study group are presented in Fig. 1.

Surgical Procedures

Anesthesia was induced via inhalation of 4% isoflurane and then maintained at 2% for the duration of surgery. In the right eye, a lateral conjunctival peritomy was performed, and the optic nerve was exposed by blunt dissection. Next, an atraumatic microvascular clamp (Fine Science Tools, North Vancouver, BC, Canada) was used to occlude the ophthalmic vessels and compress the optic nerve <1mm from the posterior eye. Prior to removing the clamp for reperfusion, complete ischemia was documented by retinal imaging and visualization of severely narrowed retinal arteries. Sham surgery included exposure of the optic nerve, but no clamp was applied. Isoflurane was discontinued upon completion of the surgery. Anesthesia was administered and maintained via intraperitoneal injection of ketamine (100 mg/kg) and xylazine (5 mg/kg) during imaging and ERG procedures.

Prior to imaging, the femoral artery was cannulated to administer Pd-porphine (an oxygen-sensitive molecular probe; 20 mg/kg) and 2-μm polystyrene fluorescent microspheres (107 particles/ml 0.9% saline) (Life Technologies, Eugene, OR) for blood velocity imaging.

Pupils were dilated using phenylephrine 2.5% (Paragon, Portland, OR) and tropicamide 1% (Bausch and Lomb, Tampa, FL). Hypromellose (0.3%) lubricant eye gel (GenTeal gel, Ciba Vision, Duluth, GA, USA; Ciba Vision, Duluth, GA, USA) was applied to the eyes, and a glass cover slip was placed on the corneas to minimize their refractive powers and prevent dehydration during imaging.

Vascular Oxygen and Blood Flow Imaging

Retinal vascular oxygen tension (PO_2) was measured using our phosphorescence lifetime imaging system as described previously (Blair et al., 2018; Wanek et al., 2011; Wanek et al., 2013, 2014). Briefly, in retinal vessels, phosphorescence lifetime of Pd-porphine (excitation at 532 nm and emission filter transmission > 645 nm) was determined using a frequency-domain approach, and the Stern-Volmer equation was used to convert these results to PO_2 measurements. Using the rat hemoglobin dissociation curve (Cartheuser, 1993), arterial and venous oxygen saturation was calculated from mean PO_2, values separately averaged in all arteries and veins. Summing oxygen bound to hemoglobin and dissolved in blood was used to determine arterial (O_{2A}) and venous (O_{2V}) oxygen contents. Arteriovenous oxygen content difference (O_{2AV}) was calculated as O_{2A}-O_{2V}. As previously described (Blair et al., 2018; Wanek et al., 2011; Wanek et al., 2013, 2014), venous blood velocity (V) was determined by analyzing a sequence of images to measure the displacement of fluorescent microspheres (excitation at 488 nm and emission filter transmission 560 ± 60 nm) over time. Red free retinal images were used to measure venous blood vessel diameter (D). Blood flow ($V\pi D^2/4$) was calculated for each vein and then summed over all veins to derive the total retinal blood flow (TRBF). Retinal DO_2, MO_2, and OEF were calculated using the following equations: DO_2 = TRBF x O_{2A}, MO_2 = TRBF x O_{2AV}, OEF = MO_2/DO_2.

Electroretinography

Two-hour dark-adapted rats underwent scotopic ERG testing (Handheld Multi-species-ElectroRetinoGraph (HMsERG, Ocuscience, Kansas City, MO, USA). As described previously (Matei et al., 2020), a ground electrode was placed in tail skin, the reference needle electrodes were placed below each eye, and contact lenses with gold-embedded electrodes (MAYO Corporation, Japan) were placed on the corneas using a conductance medium (GenTeal). ERG a- and b-wave amplitudes at a flash intensity of 1 cd s/m^2 were measured.

Biochemical Evaluations

Immunofluorescence staining was performed as previously described (Zheng et al., 2019). Briefly, fixed retinal sections were deparaffinized, boiled in a citrate antigen retrieval buffer (10 mM Sodium Citrate, 0.05% Tween 20, pH 6.0) for 20 min, blocked with 10% normal donkey serum, incubated overnight with the primary antibodies rabbit anti-GFAP (1:200; ab7260, RRID:AB_305808), and incubated with a secondary antibody conjugated with FITC and then 4′,6-diamidino-2-phenylindole, dihydrochloride (DAPI) (nuclear marker, color blue). No staining was observed in the imaging of the negative control, in which the primary antibody was omitted.

Terminal deoxynucleotidyl transferase dUTP nick and labeling (TUNEL) assay (Roche, USA) was used to evaluate cellular apoptosis. To quantify the number of TUNEL-positive cells (green) colocalized with DAPI, a researcher without knowledge of group allocation manually counted all colocalized cells throughout one retinal section. Immunoreactivity for GFAP was estimated using a previously reported grade score(Yamamoto et al., 2006): 0=no signal, 1=few positive glial endfeet in ganglion cell layer or scattered processes in other layers, 2=few labelled processes reaching from ganglion cell to outer nuclear layer, and 3=most labelled processes reaching from ganglion cell layer to the outer nuclear layer.

Spectral-Domain Optical Coherence Tomography

As described previously (Blair et al., 2019), spectral-domain OCT imaging (Spectralis, Heidelberg Engineering, Heidelberg, Germany) was performed in regions nasal and temporal to the optic nerve head. Images were analyzed using the unit's software (Heidelberg Eye Explorer 1.9.10.0; Heidelberg Engineering) to measure the total retinal thickness (TRT) which was averaged over nasal and temporal regions.

Statistical Analysis

SSPS Statistics (Version 24, IBM Armonk, New York) was used for statistical analyses. Measured data (TRBF, O_{2A}, and O_{2v}) were evaluated by group and 3 outliers (values more than three times the interquartile range) were removed. Also, data from 4 animals were removed because calculated MO_2 values were either an outlier or slightly negative, though close to the physiological lower limit of zero. Overall, data were available in 61 animals for statistical analysis. Compiled data were evaluated for normality using Shapiro-Wilk tests. Linear regression analysis was used to determine the slopes and y-intercepts of the regression lines relating MO_2, TRT, and ERG b-wave amplitude to ischemia duration. Data from sham groups imaged after 1-hour and 7-days reperfusion were combined. One-way ANOVA with post hoc Tukey HSD tests was used to determine differences in data among sham and OVO groups after 1-hour or 7-days reperfusion. Kruskal–Wallis tests were used to determine the significance of differences in GFAP scores and TUNEL-positive cells among groups. The mean rank of each column was compared with the mean rank of the sham group, and the comparisons were adjusted by Bonferroni correction for multiple tests. For all comparisons, estimates (β) of mean differences with respect to the sham group were determined. Pearson correlation (r_P = correlation coefficient) analysis was used to relate MO_2 to TRT and ERG a- and b-wave amplitudes, and Spearman's rank correlation (r_s = correlation coefficient) analysis was used to relate MO_2 with the number of TUNEL-positive cells and GFAP scores. An estimated value and impairment index for each metric (MO_2, b-wave amplitude, and TRT) were calculated according to the following steps. First, a linear regression model was used to find the best fit of the measured metric in multiple rats as a function of ischemia duration and derive the slope (m) and y-intercept (b). Second, an estimated metric was calculated at each ischemia duration using the regression parameters (m and b): estimated metric = m * ischemia duration + b. Third, the estimated metric was used to calculate an impairment Index = (b − estimated metric)/b. The values of impairment index range between 0 and 1, corresponding to no and maximum impairment, respectively. For statistical analyses, significance was accepted at $P \leq 0.05$.

RESULTS

Blood Flow and Oxygen Delivery

TRBF and DO_2 data stratified by ischemia and reperfusion durations are presented in Figure 2. TRBF was 6.4±1.5 μL/min in the sham group (N=10). After 1-hour reperfusion, TRBF was reduced in the 180-min OVO group (β= −3.5 μL/min; P=0.006). Similarly, after 7-day reperfusion, TRBF was reduced in the 180-min OVO group (β= −3.2 μL/min; P=0.02). TRBF in 60-, 90-, and 120-min OVO groups were not significantly different than the sham group after both reperfusion durations (P>0.06).

DO_2 was 824±226 nLO_2/min in the sham group (N=10). After 1-hour reperfusion, DO_2 was reduced in the 180-min (β= −426 nLO_2/min) OVO group (P=0.03). DO_2in 60-, 90-, and 120-min OVO groups were not significantly different than the sham group (P>0.06). After 7-day reperfusion, DO_2 in all OVO groups did not differ significantly from the sham group (P>0.06).

Oxygen Metabolism and Extraction Fraction

MO_2 and OEF data stratified by ischemia and reperfusion durations are presented in Figure 3. MO_2 was 369±84 nLO_2/min in the sham group (N=10). After 1-Flour reperfusion, MO_2 was reduced in 60-(β= −158 nLO_2/min), 90-(β= −305 nLO_2/min), 120-(β= −231 nLO_2/min), and 180-min (β= −351 nLO_2/min) OVO groups compared to the sham group (P< 0.001). After 7-day reperfusion, MO_2 was reduced in 90-(β= −193 nLO_2/min), 120-(β= −171 nLO_2/min), and 180-min (β= −222 nLO_2/min) OVO groups compared to the sham group (P< 0.04).

OEF was 0.45±0.07 in the sham group (N=10). After 1-hour reperfusion, OEF was reduced in 90-min (β= −0.36), 120-min (β= −0.26), and 180-min (β= −0.40 nLO_2/min) OVO groups compared to the sham group (P< 0.001). After 7-day reperfusion, OEF was reduced only in the 180-min (β= −0.20) OVO group compared to the sham group (P=0.01).

Visual Function (Electroretinography)

Mean and standard deviation of ERG a- and b-wave amplitudes obtained after 7-days of reperfusion and stratified by ischemia duration are shown in Figure 4 A and B, respectively. In the sham group, ERG a-wave and b-wave amplitudes were 96.1±35.4 μV and 493±177 μV, respectively (N=5). Compared to the sham group, ERG a-wave amplitude was reduced in the 180-min OVO group (P=0.01; N=6). No significant differences were detected in ERG a-wave amplitude in 60-, 90-, and 120-min OVO groups (P>0.5). Compared to the sham group, ERG b-wave amplitude was reduced in 90-min (β= −303 μV; N=4), 120-min (β= −367 μV; N=4) and 180-min (β= −449 μV; N=6) OVO groups (P≤0.01). No significant differences were detected in ERG b-wave amplitude in the 60-min OVO group compared to the sham group (P=0.13). Based on compiled data from all OVO groups after 7 days of reperfusion, MO_2 was linearly correlated with amplitudes of ERG a-wave (r_P=0.44; P=0.03; N=23) and b-wave (r_P=0.67; P<0.0001; N=23).

Retinal Degeneration (Gliosis and Apoptosis)

Retinal sections stained for GFAP are shown in Figure 5A. Mean and standard deviation of GFAP expression obtained after 7-day reperfusion and stratified by ischemia duration are shown in Figure 5B. There was a statistically significant difference in GFAP score among OVO groups (P=0.00004). The mean rank GFAP scores were 7.0, 7.0, 16.8, 19.2, and 21.2 for sham, 60-min, 90-min, 120-min, and 180-min OVO groups, respectively. GFAP score was higher in the 120- and 180-min OVO groups compared to the sham group (P<0.03). No significant differences were detected in the mean rank GFAP scores in 60- and 90-min OVO groups compared to the sham group (P>0.1). Based on compiled data at 7-day reperfusion, MO_2 was inversely associated with GFAP score (r_s=−0.56; P≤0.02; N=27).

Retinal sections stained for TUNEL are shown in Figure 6A. Mean and standard deviation of the number of TUNEL-positive cells measured after 7-day reperfusion and stratified by ischemia duration are shown in Figure 6B. There was a statistically significant difference in the number of TUNEL-positive cells among OVO groups (P=0.01). The mean rank number of TUNEL-positive cells was 7.5, 6.0, 16.2, 19.6, and 22.5 for sham, 60-min, 90-min, 120-min, and 180-min OVO groups, respectively. The number of TUNEL-positive cells was higher in 120- and 180- min OVO groups compared to the sham group (P≤0.04). No significant differences were detected in the number of TUNEL-positive cells in 60- and 90-min OVO groups compared to the sham group (P≥0.3). Based on compiled data from all OVO groups after 7 days of reperfusion, MO_2 was inversely associated with the number of TUNEL-positive cells (r_s =−0.69; P=0.0001; N=27).

Retinal Thickness

Mean and standard deviation of TRT obtained after 7-day reperfusion and stratified by ischemia duration are shown in Figure 7. TRT was 254±8 μm in the sham group (N=5). TRT was reduced in 120-min (β= −83 μm; N=6) and 180-min (β=−115 μm; N=6) OVO groups compared to the sham group (p≤0.02). Compared to the sham group, TRT in 60-min and 90-min OVO groups were not significantly different (P≥0.1; N=6). Based on compiled in all OVO groups after 7 days of reperfusion, MO_2 was linearly related to TRT (r_P=−0.72; P0.0001; N=29).

Prognostic Value of MO_2

After 1-hour reperfusion, MO_2 was linearly related to the duration of ischemia (R=0.82; P<0.001; N=35). Similarly, after 7-days of reperfusion, there were linear relationships of b-wave amplitude (R=0.82; P<0.001; N=23) and TRT (R=0.72; P<0.001; N=29) with ischemia duration. The y-intercepts (b) and slopes (m) of the regression lines are reported in Table 1.

Figure 8 shows the relationships of b-wave amplitude and TRT impairment indices after 7-days reperfusion to MO_2 impairment index after 1-hour reperfusion. Since the plot is based on calculated (not measured) metrics, error bars are not shown. Based on linear regression models, the estimated impairments in b-wave amplitude and TRT outcomes were 0.97 and 0.46 times the impairment in MO_2 shortly after ischemia/reperfusion injury, respectively.

DISCUSSION

In the present study, we confirmed our first hypothesis that after ischemia followed by 7 days of reperfusion, MO_2 reduction is related to visual dysfunction, retinal thinning, and increased gliosis and cell loss. We also confirmed our second hypothesis that MO_2 impairment shortly after ischemia/reperfusion predicted impairments in visual function and retinal thickness outcomes after 7 days of reperfusion.

Retinal Blood Flow and Oxygen Delivery

During OVO, there is complete obstruction of blood flow, such that both TRBF and DO_2 = 0. As the duration of reperfusion increases, TRBF and DO_2 are expected to gradually increase with time. Indeed after 1 hour of reperfusion, we observed TRBF and DO_2 recovery to sham values with ischemia durations less than 180 minutes. This expectation was confirmed in our previous study in which after 120 minutes of ischemia followed by 20 minutes of reperfusion, TRBF and DO_2 had not yet recovered (Blair et al., 2019). Given that the retina consumes oxygen rapidly, under conditions of reduced TRBF and DO_2 with ischemia durations of 180 minutes or more, the supply of metabolites (oxygen and glucose) needed for cellular function and survival are reduced. This results in the depletion of minimal energy reserves and eventual cell death if oxygen supply is not restored (Kaur et al., 2008). Oxygen continues to drive the most energy-producing pathway in cells, oxidative phosphorylation, and during ischemia, glucose metabolism is shifted towards less efficient anaerobic glycolytic pathways (Maltepe and Saugstad, 2009).

Retinal Oxygen Metabolism

MO_2 was reduced after ischemia durations of 60 minutes or more and 1-hour reperfusion and recovered to sham values only after 60 minutes of ischemia and 7-day reperfusion duration. The finding of MO_2 reduction may be attributed to at least one of three factors: transient metabolic inactivity that may be regained with reperfusion, cell death, and increased oxygen availability from the choroidal circulation. First, our finding of restored MO_2 after 60-min ischemia and 7-day reperfusion suggests transient metabolic inactivity. It is known that before undergoing cell-death, cerebral tissue may exhibit electrical failure (Markus, 2004). In efforts to maintain cellular survival and metabolism, endogenous phosphocreatine is initially used to generate ATP, but as oxygen levels are further reduced, glycolytically metabolized glucose increases levels of lactate, which is associated with a decrease in pH (Sims and Muyderman, 2010). Literature has shown that after 120 minutes of ischemia in the brain, phosphocreatine levels were reduced by 70% compared to non-ischemic tissue, which resulted in a ~50% reduction in ATP levels. However, with ischemia durations below 120 minutes, recovery of both phosphocreatine and adenylate energy were observed after just two hours of reperfusion (Folbergrova et al., 1995). These studies suggest that as glucose and oxygen continue to be supplied, metabolic activity may be regained as long as irreversible energy pathways were not activated.

Second, it is reasonable to conclude that the observed reduction in MO_2 after 7-days reperfusion may be partially attributed to cell-death, which occurs after energy depletion and subsequent plasma membrane compromise (D'Onofrio and Koeberle, 2013). Specifically,

it is known that when blood flow is completely extinguished, levels of ATP may be reduced to very low levels within minutes, and if they are not restored with reperfusion, irreversible energy failure ensues (cell-death): ionic gradients across the plasma membrane are neutralized, such that intracellular potassium is reduced, while intracellular calcium is increased (Doyle et al., 2008). This conclusion is also supported by our findings of decreased TRT and increased number TUNEL-positive cells.

Third, the finding of reduced MO_2 (rate of oxygen extracted from the retinal circulation) after 7-days of reperfusion may be partially attributed to increased oxygen delivery from the choroidal circulation due to decreased photoreceptor oxygen consumption. In literature, there is evidence of photoreceptor cell death due to ischemia/reperfusion and increased choroidal oxygen availability due to photoreceptor degeneration. In an elevated intraocular pressure (IOP) ischemia/reperfusion rat model, photoreceptor cell death was observed after an ischemia duration of 60 minutes, as early as 12 hours and continued up to 7 days following reperfusion (Palmhof et al., 2019). Moreover, in a photoreceptor degenerative Abyssinian cat model, oxygen from the choroid was able to reach and supply the inner retina, maintaining inner retinal PO_2 near normal levels as the retinal circulation was attenuated (Padnick-Silver et al., 2006). The finding of statistically significant reduction of the a-wave only with 180 minutes of ischemia suggests that the photoreceptors were not as severely affected.

Retinal Oxygen Extraction Fraction

Given that literature has shown OEF to be a reliable indicator for adequacy of oxygen supply for metabolism (Blair et al., 2019; Shahidi et al., 2018; Teng et al., 2013), it may also be indicative of retinal function. OEF was reduced at ischemia durations ≥ 90 minutes and 180 minutes after 1-hour and 7-day reperfusion, respectively. With a maintained DO_2 at 7-day reperfusion, the reduction in OEF may be primarily attributed to decreased MO_2 due to permanent cell loss, transient metabolic inactivity or increased oxygen availability from the choroidal circulation. An increase in OEF after 120 minutes of ischemia and 20 minutes of reperfusion was reported by Blair et al (Blair et al., 2019) resulting predominately from a low level of DO_2. After 90 minutes of ischemia, reduced OEF after 1 hour of reperfusion was coupled with increased tissue damage (reduced TRT) after 7 days of reperfusion. This is consistent with a previous finding in a monkey model of cerebral ischemia that showed reduced OEF that was related to an increase in cortical damage (cell loss) (Takamatsu et al., 2000).

Retinal Visual Function (Electroretinography)

In the current study, ERG b-wave amplitude was inversely related with ischemia duration, in agreement with the finding of a previous study (Block and Schwarz, 1998). Mechanistically, retinal ischemia increases levels of excitatory amino acids, such as glutamate and aspartate, which disturb calcium homeostasis in Muller cells and thereby attenuate b-wave amplitudes (Block and Schwarz, 1998). In addition, choroidal hypoperfusion resulting from OVO may cause damage to the photoreceptors and hence attenuate a- and b-wave amplitudes. Furthermore, our finding of reduction in ERG b-wave amplitudes at ischemia durations ≥ 90 minutes is consistent with studies that showed near normal and reduced ERG

b-wave amplitudes after reperfusion and ischemia durations ≤ 60 minutes (Gehlbach and Purple, 1994) and ≥ 90 minutes (Braun and Linsenmeier, 1995; Hayreh et al., 2004; Kroll, 1968), respectively. Our finding of sustained ERG a-wave amplitudes after ischemia duration < 180 minutes is in agreement with a previous study which reported normal ERG a-wave amplitudes with ischemia durations ≤ 90-minutes at 7-days of reperfusion (Mayor-Torroglosa et al., 2005).

Given the sensitivity of neurons, literature has shown the retina and visual system to be very susceptible to ischemia (Wong-Riley, 2010). As expected, MO_2 was linearly related to both ERG a- and b-wave amplitudes. In agreement with our study, in a bilateral common carotid artery occlusion rat incomplete ischemia model, we also reported reduced MO_2 to be related with reduced ERG b- wave amplitude (Matei et al., 2020).

Retinal Degeneration (Gliosis and Apoptosis)

In the current study, GFAP score was increased with ischemia durations ≥ 120 minutes. Gliosis can be a sensitive, early indicator of ischemia induced damage (de Hoz et al., 2016). Reactive gliosis and Muller cell activation are reflected in the GFAP score determined in the current study. In elevated IOP ischemia/reperfusion pig (Wurm et al., 2011) and rat (Luo et al., 2018) models, after ischemia durations of 60 minutes or more and 3 days of reperfusion, GFAP immunoreactivity was increased, indicating hypertrophy of gliotic Muller cells. Muller cells are the chief glial cells in the retina and support neurons with blood-derived nutrients (Bringmann et al., 2006), but after severe ischemia, they secrete factors such as matrix metalloproteinases (Behzadian et al., 2001; Milenkovic et al., 2003) that lead to the eventual degradation of the blood-retinal barrier (BRB). The BRB is responsible for the transport of macromolecules, and when the homeostatic retinal microenvironment is compromised through BRB failure, visual dysfunction and increased damage may ensue (Xu and Le, 2011).

In the current study, an increase in the number of TUNEL-positive apoptotic cells was detected after ischemia duration ≥ 120 minutes followed by 7 days of reperfusion, suggesting reperfusion injury may have played a role in exacerbating injury and cell-death via apoptosis. In an elevated IOP ischemia/reperfusion rat model, under ischemia durations greater than 90 minutes, it was shown that the first phase of cell-death typically results from necrosis. This is followed by a second phase of neuronal death via activation of apoptotic pathways (Joo et al., 1999). Specifically, necrosis is a fast cellular-death process that occurs as a result of membrane failure and subsequently results in inflammation and toxic activation of phagocytes (Dvoriantchikova et al., 2010). In contrast, apoptosis is an energy-dependent, regulated, and programed cell-death process, resulting in minimal damage to surrounding cells, and taking hours to days to complete (Broughton et al., 2009). Therefore, prolonged periods of ischemia increase the initial rate of necrosis, and reperfusion injury may further increase cell loss by apoptosis via restoration of energy required to complete this process (Dumont et al., 2001; Gottlieb et al., 1994). Future studies are needed to characterize the relationship of apoptosis and necrosis in the OVO model of retinal ischemia.

MO_2 was found to be related to retinal degeneration markers of gliosis and apoptosis. The current study showed an inverse association between MO_2 and GFAP score. Although

studies have shown astrogliosis to correlate with infarct size in the brain (Wang et al., 2008), there is a lack of research correlating the level of gliosis to tissue metabolism. The observation of reduced MO_2 and visual dysfunction in the current study may be attributed in part to increased neuronal degeneration induced by increased gliosis (Vazquez-Chona et al., 2011), as has been previously reported in a POMGnT1-deficient mouse model (Takahashi et al., 2011). Therefore, gliosis develops in synchrony with reductions in MO_2. An inverse association between MO_2 and number of TUNEL-positive cells was observed in the current study. Mehmet et al. showed apoptotic cells were linearly related to the severity of reduced cerebral energy metabolism (Mehmet et al., 1998).

Retinal Thickness

TRT and ischemia duration were inversely related, and a reduction in TRT occurred after ischemia durations ≥ 120 minutes and 7 days of reperfusion. This finding is consistent with reported results in an ophthalmic artery occlusion rhesus monkey model after ischemia durations ≥105 minutes and 13-16 weeks of reperfusion (Hayreh et al., 1980). On the other hand, in an elevated IOP ischemia/reperfusion rat model, decreased TRT was reported after 90 minutes of ischemia and 7 days of reperfusion (Sho et al., 2005). The detection of retinal thinning at a shorter duration of ischemia compared to our findings is likely due the potential of tissue damage under elevated IOP condition from both mechanical and ischemic factors. In fact, these factors were proposed to be independent (He et al., 2013). The increase in TRT that we reported previously after 120 minutes of ischemia and 20 minutes of reperfusion (Blair et al., 2019) occurs presumably prior to subsequent retinal thinning with longer reperfusion duration shown in the current study. This sequence of initial thickening due to cytotoxic edema resulting from impaired Na+/K+ -ATPase pump activity with subsequent thinning also has been documented in the inner retina in human branch retinal artery occlusion (Ritter et al., 2012).

Reduced TRT was associated with decreased MO_2 after 7-days reperfusion. As ischemia duration increases, cells that primarily rely on oxidative metabolism, such as neurons of the inner retina, are the first to be compromised. In detail, in neurons, the highest energy-consuming functions predominately include the active transport of ions that establish the transmembrane ionic gradient (Ames et al., 1992; Niven and Laughlin, 2008; Wong-Riley, 2010). Ischemic depletion of energy will lead to cell death. Energy dependent apoptotic pathways are then activated when reperfusion occurs, leading to cell-death (Wong-Riley, 2010). With a decrease in the number of cells, both the thickness of the retina and MO_2 are expected to be permanently reduced.

Prognostic Value of MO_2

Since MO_2 reflects energy metabolism which underlies numerous cellular processes, it shows promise as a biomarker to predict outcomes after ischemia. Clinically, patients with severe levels and long durations of ischemia are known to have less favorable outcomes. However, determining the prognosis of patients with moderate levels of ischemia currently remains unsatisfactory. Recent studies showed retinal oximetry is not predictive of visual outcome after anti-VEGF treatment for retinal vein occlusion (Jeppesen and Bek, 2017, 2021; Krejberg Jeppesen et al., 2021). However, the prognostic value of MO_2 which

incorporates the coupling of arteriovenous oxygen saturation and blood flow has not been previously investigated. In the current study, for the first time, MO_2 measured after 1 hour of reperfusion was shown to predict ERG b-wave amplitude and TRT outcomes after 7 days of reperfusion. Interestingly, there was an almost one to one correspondence between impairment of MO_2 immediately after injury and visual function impairment outcome after 7 days of reperfusion. Since MO_2 can be measured in humans, future studies are needed to investigate its potential to serve as a biomarker for predicting outcomes and assessing interventions following ischemia/reperfusion injury.

Limitations

There are several limitations of this work. First, the procedure for OVO used a clamp for vessel occlusion was similar to the one reported by Stefánsson et al. (Stefánsson et al., 1988) but different from those reported by LaFuente et al. (Lafuente et al., 2002) and Blair et al. (Blair et al., 2019). The clamp may have damaged nerve fiber layer axons. However, the closing force of the clamp was set by the manufacturer to a pressure that is assumed to be non-traumatic to blood vessels, thus minimizing the mechanical damage. Nevertheless, given the use of an experimental model of ischemia/reperfusion and differences in vascular re-perfusion responses between rats and humans, translation of findings to human vascular occlusive conditions may be limited. Overall, the findings may not be generalizable to animals of different age, sex, or species. Second, since choroidal blood flow was not measured, the level of choroidal recovery after reperfusion and the extent of attenuation in MO_2 resulting from increased oxygen supply from the choroid are unknown. Third, the prognostic value of MO_2 was determined with the use of a linear mathematical model as a first approximation. Given recovery has been reported up to 100 minutes after ischemia in a rhesus monkey model of ischemia/reperfusion” (Hayreh et al., 1980), it is conceivable that the relationship between MO_2 and ischemia duration may be nonlinear, such that MO_2 may remain initially unchanged at low durations of ischemia. Fourth, there may have been variations in the unmonitored blood pressure of rats, though there was no significant difference in the heart rates among groups. Fifth, small sample sizes (low statistical power) may have increased the probability of a type two error, such that no statistically significant difference in means would be found when one actually was present. Sixth, a constant hemoglobin concentration was assumed for calculation of oxygen contents under both normal and reduced blood flow conditions. A previous study (McHedlishvili and Varazashvili, 1987), showed a reduction of 52% in cerebral blood flow resulted in a ~20% reduction in the number of red blood cells and hematocrit levels in pial veins due to the Fahraeus effect. Given TRBF was reduced by approximately 50% in only the 180-min OVO group, oxygen contents, DO_2 and MO_2 values may have been overestimated. Accounting for this overestimation does not affect the reported results of reductions in DO_2 after 1-hour reperfusion and in MO_2 after both reperfusion durations. However, DO_2 after 7-day reperfusion may have been reduced, though not recognized in the current study.

CONCLUSION

In conclusion, reduction in MO_2 was correlated with visual dysfunction and retinal thinning after ischemia and 7 days of reperfusion and MO_2 impairment shortly after reperfusion

was predictive of visual function and retinal thickness impairment outcomes after 7 days of reperfusion. Taken together, these findings advance our understanding of the pathophysiology of retinal ischemia/reperfusion and suggest the potential prognostic value of MO_2.

Acknowledgements:

The authors thank James Burford for performing animal procedures.

Funding

This work was supported by NEI grants, EY017918 and EY029220, and Research to Prevent Blindness Foundation.

References

Aanerud J, Borghammer P, Chakravarty MM, Vang K, Rodell AB, Jonsdottir KY, Moller A, Ashkanian M, Vafaee MS, Iversen P, Johannsen P, Gjedde A, 2012. Brain energy metabolism and blood flow differences in healthy aging. J Cereb Blood Flow Metab 32, 1177–1187. [PubMed: 22373642]

Ames A 3rd, Li YY, Heher EC, Kimble CR, 1992. Energy metabolism of rabbit retina as related to function: high cost of Na+ transport. J Neurosci 12, 840–853. [PubMed: 1312136]

An H, Ford AL, Chen Y, Zhu H, Ponisio R, Kumar G, Shanechi AM, Khoury N, Vo KD, Williams J, Derdeyn CP, Diringer MN, Panagos P, Powers WJ, Lee JM, Lin W, 2015. Defining the Ischemic Penumbra using Magnetic Resonance Oxygen Metabolic Index. Stroke 46, 982–988. [PubMed: 25721017]

Behzadian MA, Wang XL, Windsor LJ, Ghaly N, Caldwell RB, 2001. TGF-beta increases retinal endothelial cell permeability by increasing MMP-9: possible role of glial cells in endothelial barrier function. Invest Ophthalmol Vis Sci 42, 853–859. [PubMed: 11222550]

Bhisitkul RB, Robinson GS, Moulton RS, Claffey KP, Gragoudas ES, Miller JW, 2005. An antisense oligodeoxynucleotide against vascular endothelial growth factor in a nonhuman primate model of iris neovascularization. Arch Ophthalmol 123, 214–219. [PubMed: 15710818]

Blair NP, Felder AE, Tan MR, Shahidi M, 2018. A Model for Graded Retinal Ischemia in Rats. Transl Vis Sci Technol 7, 10.

Blair NP, Tan MR, Felder AE, Shahidi M, 2019. Retinal oxygen delivery, metabolism and extraction fraction and retinal thickness immediately following an interval of ophthalmic vessel occlusion in rats. Sci Rep 9, 8092. [PubMed: 31147557]

Block F, Schwarz M, 1998. The b-wave of the electroretinogram as an index of retinal ischemia. Gen Pharmacol 30, 281–287. [PubMed: 9510075]

Braun RD, Linsenmeier RA, 1995. Retinal oxygen tension and the electroretinogram during arterial occlusion in the cat. Invest Ophthalmol Vis Sci 36, 523–541. [PubMed: 7890484]

Bringmann A, Pannicke T, Grosche J, Francke M, Wiedemann P, Skatchkov SN, Osborne NN, Reichenbach A, 2006. Muller cells in the healthy and diseased retina. Prog Retin Eye Res 25, 397–424. [PubMed: 16839797]

Broughton BR, Reutens DC, Sobey CG, 2009. Apoptotic mechanisms after cerebral ischemia. Stroke 40, e331–339. [PubMed: 19182083]

Cartheuser CF, 1993. Standard and pH-affected hemoglobin-O2 binding curves of Sprague-Dawley rats under normal and shifted P50 conditions. Comp Biochem Physiol Comp Physiol 106, 775–782. [PubMed: 7906635]

D'Onofrio PM, Koeberle PD, 2013. What can we learn about stroke from retinal ischemia models?, Acta Pharmacol Sin, pp. 91–103. [PubMed: 23202803]

de Hoz R, Rojas B, Ramírez AI, Salazar JJ, Gallego BI, Triviño A, Ramírez JM, 2016. Retinal Macroglial Responses in Health and Disease. Biomed Res Int 2016.

Dominguez E, Raoul W, Calippe B, Sahel JA, Guillonneau X, Paques M, Sennlaub F, 2015. Experimental Branch Retinal Vein Occlusion Induces Upstream Pericyte Loss and Vascular Destabilization. PLOS ONE 10, e0132644. [PubMed: 26208283]

Doyle KP, Simon RP, Stenzel-Poore MP, 2008. Mechanisms of ischemic brain damage. Neuropharmacology 55, 310–318. [PubMed: 18308346]

Dumont EA, Reutelingsperger CP, Smits JF, Daemen MJ, Doevendans PA, Wellens HJ, Hofstra L, 2001. Real-time imaging of apoptotic cell-membrane changes at the single-cell level in the beating murine heart. Nat Med 7, 1352–1355. [PubMed: 11726977]

Dvoriantchikova G, Barakat DJ, Hernandez E, Shestopalov VI, Ivanov D, 2010. Liposome-delivered ATP effectively protects the retina against ischemia-reperfusion injury. Mol Vis 16, 2882–2890. [PubMed: 21203410]

Ebneter A, Kokona D, Schneider N, Zinkernagel MS, 2017. Microglia Activation and Recruitment of Circulating Macrophages During Ischemic Experimental Branch Retinal Vein Occlusion. Invest Ophthalmol Vis Sci 58, 944–953. [PubMed: 28170538]

Folbergrova J, Zhao Q, Katsura K, Siesjo BK, 1995. N-tert-butyl-alpha-phenylnitrone improves recovery of brain energy state in rats following transient focal ischemia. Proc Natl Acad Sci U S A 92, 5057–5061. [PubMed: 7761448]

Fry BC, Coburn EB, Whiteman S, Harris A, Siesky B, Arciero J, 2018. Predicting retinal tissue oxygenation using an image-based theoretical model. Math Biosci 305, 1–9. [PubMed: 30149022]

Gehlbach PL, Purple RL, 1994. A paired comparison of two models of experimental retinal ischemia. Curr Eye Res 13, 597–602. [PubMed: 7956312]

Genevois O, Paques M, Simonutti M, Sercombe R, Seylaz J, Gaudric A, Brouland JP, Sahel J, Vicaut E, 2004. Microvascular remodeling after occlusion-recanalization of a branch retinal vein in rats. Invest Ophthalmol Vis Sci 45, 594–600. [PubMed: 14744903]

Gottlieb RA, Burleson KO, Kloner RA, Babior BM, Engler RL, 1994. Reperfusion injury induces apoptosis in rabbit cardiomyocytes. J Clin Invest 94, 1621–1628. [PubMed: 7929838]

Hayreh SS, 2001. Blood Flow in the Optic Nerve Head and Factors that may Influence it. Progress in Retinal and Eye Research 20, 595–624. [PubMed: 11470452]

Hayreh SS, Kolder HE, Weingeist TA, 1980. Central retinal artery occlusion and retinal tolerance time. Ophthalmology 87, 75–78. [PubMed: 6769079]

Hayreh SS, Zimmerman MB, Kimura A, Sanon A, 2004. Central retinal artery occlusion. Retinal survival time. Exp Eye Res 78, 723–736. [PubMed: 15106952]

He Z, Lim JK, Nguyen CT, Vingrys AJ, Bui BV, 2013. Coupling blood flow and neural function in the retina: a model for homeostatic responses to ocular perfusion pressure challenge. Physiol Rep 1, e00055. [PubMed: 24303137]

Jeppesen SK, Bek T, 2017. Retinal Oxygen Saturation Correlates With Visual Acuity but Does Not Predict Outcome After Anti-VEGF Treatment in Central Retinal Vein Occlusion. Invest Ophthalmol Vis Sci 58, 2498–2502. [PubMed: 28470332]

Jeppesen SK, Bek T, 2021. Lack of predictive value of retinal oxygen saturation for visual outcome after angiostatic treatment of branch retinal vein occlusion. Acta Ophthalmol doi: 10.1111/aos.14988.

Joo CK, Choi JS, Ko HW, Park KY, Sohn S, Chun MH, Oh YJ, Gwag BJ, 1999. Necrosis and apoptosis after retinal ischemia: involvement of NMDA-mediated excitotoxicity and p53. Invest Ophthalmol Vis Sci 40, 713–720. [PubMed: 10067975]

Kaur C, Foulds WS, Ling EA, 2008. Hypoxia-ischemia and retinal ganglion cell damage. Clin Ophthalmol 2, 879–889. [PubMed: 19668442]

Krejberg Jeppesen S, Sin M, Hakon Hardarson S, Bek T, 2021. Retinal oximetry does not predict 12-month visual outcome after anti-VEGF treatment for central retinal vein occlusion: A multicentre study. Acta Ophthalmol 99, e1141–e1145. [PubMed: 33421320]

Kroll AJ, 1968. Experimental central retinal artery occlusion. Arch Ophthalmol 79, 453–469. [PubMed: 4966522]

Lafuente MP, Villegas-Perez MP, Selles-Navarro I, Mayor-Torroglosa S, Miralles de Imperial J, Vidal-Sanz M, 2002. Retinal ganglion cell death after acute retinal ischemia is an ongoing process whose

severity and duration depends on the duration of the insult. Neuroscience 109, 157–168. [PubMed: 11784707]

Leske MC, Heijl A, Hyman L, Bengtsson B, Dong L, Yang Z, 2007. Predictors of Long-term Progression in the Early Manifest Glaucoma Trial. Ophthalmology 114, 1965–1972. [PubMed: 17628686]

Luo H, Zhuang J, Hu P, Ye W, Chen S, Pang Y, Li N, Deng C, Zhang X, 2018. Resveratrol Delays Retinal Ganglion Cell Loss and Attenuates Gliosis-Related Inflammation From Ischemia-Reperfusion Injury. Invest Ophthalmol Vis Sci 59, 3879–3888. [PubMed: 30073348]

Maltepe E, Saugstad OD, 2009. Oxygen in health and disease: regulation of oxygen homeostasis--clinical implications. Pediatr Res 65, 261–268. [PubMed: 18852690]

Markus HS, 2004. Cerebral perfusion and stroke. J Neurol Neurosurg Psychiatry 75, 353–361. [PubMed: 14966145]

Matei N, Leahy S, Auvazian S, Thomas B, Blair NP, Shahidi M, 2020. Relation of Retinal Oxygen Measures to Electrophysiology and Survival Indicators after Permanent, Incomplete Ischemia in Rats. Transl Stroke Res 11, 1273–1286. [PubMed: 32207038]

Mayor-Torroglosa S, De la Villa P, Rodriguez ME, Lopez-Herrera MP, Aviles-Trigueros M, Garcia-Aviles A, de Imperial JM, Villegas-Perez MP, Vidal-Sanz M, 2005. Ischemia results 3 months later in altered ERG, degeneration of inner layers, and deafferented tectum: neuroprotection with brimonidine. Invest Ophthalmol Vis Sci 46, 3825–3835. [PubMed: 16186370]

McHedlishvili G, Varazashvili M, 1987. Hematocrit in cerebral capillaries and veins under control and ischemic conditions. J Cereb Blood Flow Metab 7, 739–744. [PubMed: 3693429]

Mehmet H, Yue X, Penrice J, Cady E, Wyatt JC, Sarraf C, Squier M, Edwards AD, 1998. Relation of impaired energy metabolism to apoptosis and necrosis following transient cerebral hypoxia-ischaemia. Cell Death Differ 5, 321–329. [PubMed: 10200478]

Milenkovic I, Weick M, Wiedemann P, Reichenbach A, Bringmann A, 2003. P2Y receptor-mediated stimulation of Muller glial cell DNA synthesis: dependence on EGF and PDGF receptor transactivation. Invest Ophthalmol Vis Sci 44, 1211–1220. [PubMed: 12601051]

Moore D, Harris A, WuDunn D, Kheradiya N, Siesky B, 2008. Dysfunctional regulation of ocular blood flow: A risk factor for glaucoma? Clin Ophthalmol 2, 849–861. [PubMed: 19668439]

Moren H, Undren P, Gesslein B, Olivecrona GK, Andreasson S, Malmsjo M, 2009. The porcine retinal vasculature accessed using an endovascular approach: a new experimental model for retinal ischemia. Invest Ophthalmol Vis Sci 50, 5504–5510. [PubMed: 19516013]

Niven JE, Laughlin SB, 2008. Energy limitation as a selective pressure on the evolution of sensory systems. J Exp Biol 211, 1792–1804. [PubMed: 18490395]

Osborne NN, Casson RJ, Wood JPM, Chidlow G, Graham M, Melena J, 2004. Retinal ischemia: mechanisms of damage and potential therapeutic strategies. Progress in Retinal and Eye Research 23, 91–147. [PubMed: 14766318]

Padnick-Silver L, Kang Derwent JJ, Giuliano E, Narfstrom K, Linsenmeier RA, 2006. Retinal oxygenation and oxygen metabolism in Abyssinian cats with a hereditary retinal degeneration. Invest Ophthalmol Vis Sci 47, 3683–3689. [PubMed: 16877443]

Palmhof M, Frank V, Rappard P, Kortenhorn E, Demuth J, Biert N, Stute G, Dick HB, Joachim SC, 2019. From Ganglion Cell to Photoreceptor Layer: Timeline of Deterioration in a Rat Ischemia/Reperfusion Model. Front Cell Neurosci 13, 174. [PubMed: 31133806]

Pournaras CJ, 1995. Retinal oxygen distribution. Its role in the physiopathology of vasoproliferative microangiopathies. Retina 15, 332–347. [PubMed: 8545580]

Ritter M, Sacu S, Deak GG, Kircher K, Sayegh RG, Pruente C, Schmidt-Erfurth UM, 2012. In vivo identification of alteration of inner neurosensory layers in branch retinal artery occlusion, Br J Ophthalmol, pp. 201–207.

Schmid H, Renner M, Dick HB, Joachim SC, 2014. Loss of inner retinal neurons after retinal ischemia in rats. Invest Ophthalmol Vis Sci 55, 2777–2787. [PubMed: 24699380]

Shabanzadeh AP, D'Onofrio PM, Monnier PP, Koeberle PD, 2018. Neurosurgical Modeling of Retinal Ischemia–Reperfusion Injury. Journal of Stroke and Cerebrovascular Diseases 27, 845–856. [PubMed: 29196198]

Shahidi M, Felder AE, Tan O, Blair NP, Huang D, 2018. Retinal Oxygen Delivery and Metabolism in Healthy and Sickle Cell Retinopathy Subjects. Invest. Ophthalmol. Vis. Sci 59, 1905–1909. [PubMed: 29677351]

Sho K, Takahashi K, Fukuchi T, Matsumura M, 2005. Quantitative evaluation of ischemia-reperfusion injury by optical coherence tomography in the rat retina. Jpn J Ophthalmol 49, 109–113. [PubMed: 15838726]

Sims NR, Muyderman H, 2010. Mitochondria, oxidative metabolism and cell death in stroke. Biochim Biophys Acta 1802, 80–91. [PubMed: 19751827]

Stefánsson E, Wilson CA, Schoen T, Kuwabara T, 1988. Experimental ischemia induces cell mitosis in the adult rat retina. Invest. Ophthalmol. Vis. Sci 29, 1050–1055. [PubMed: 3417399]

Stitt AW, O'Neill CL, O'Doherty MT, Archer DB, Gardiner TA, Medina RJ, 2011. Vascular stem cells and ischaemic retinopathies. Progress in Retinal and Eye Research 30, 149–166. [PubMed: 21352947]

Sun C, Li XX, He XJ, Zhang Q, Tao Y, 2013. Neuroprotective effect of minocycline in a rat model of branch retinal vein occlusion. Exp Eye Res 113, 105–116. [PubMed: 23748101]

Takahashi H, Kanesaki H, Igarashi T, Kameya S, Yamaki K, Mizota A, Kudo A, Miyagoe-Suzuki Y, Takeda S, 2011. Reactive gliosis of astrocytes and Muller glial cells in retina of POMGnT1-deficient mice. Mol Cell Neurosci 47, 119–130. [PubMed: 21447391]

Takamatsu H, Tsukada H, Kakiuchi T, Nishiyama S, Noda A, Umemura K, 2000. Detection of reperfusion injury using PET in a monkey model of cerebral ischemia. J Nucl Med 41, 1409–1416. [PubMed: 10945535]

Teng PY, Wanek J, Blair NP, Shahidi M, 2013. Inner retinal oxygen extraction fraction in rat. Invest Ophthalmol Vis Sci 54, 647–651. [PubMed: 23299486]

Touzani O, Young AR, Derlon JM, Baron JC, MacKenzie ET, 1997. Progressive impairment of brain oxidative metabolism reversed by reperfusion following middle cerebral artery occlusion in anaesthetized baboons. Brain Res 767, 17–25. [PubMed: 9365011]

Vazquez-Chona FR, Swan A, Ferrell WD, Jiang L, Baehr W, Chien WM, Fero M, Marc RE, Levine EM, 2011. Proliferative reactive gliosis is compatible with glial metabolic support and neuronal function. BMC Neurosci 12, 98. [PubMed: 21985191]

Verro P, Chow M, 2009. Prolonged dependence of ischemic penumbra on induced hypertension. Neurologist 15, 296–297. [PubMed: 19741441]

Wanek J, Teng PY, Albers J, Blair NP, Shahidi M, 2011. Inner retinal metabolic rate of oxygen by oxygen tension and blood flow imaging in rat. Biomed Opt Express 2, 2562–2568. [PubMed: 21991548]

Wanek J, Teng PY, Blair NP, Shahidi M, 2013. Inner retinal oxygen delivery and metabolism under normoxia and hypoxia in rat. Invest Ophthalmol Vis Sci 54, 5012–5019. [PubMed: 23821203]

Wanek J, Teng PY, Blair NP, Shahidi M, 2014. Inner retinal oxygen delivery and metabolism in streptozotocin diabetic rats. Invest Ophthalmol Vis Sci 55, 1588–1593. [PubMed: 24550355]

Wang W, Redecker C, Yu ZY, Xie MJ, Tian DS, Zhang L, Bu BT, Witte OW, 2008. Rat focal cerebral ischemia induced astrocyte proliferation and delayed neuronal death are attenuated by cyclin-dependent kinase inhibition. J Clin Neurosci 15, 278–285. [PubMed: 18207409]

Wong-Riley MT, 2010. Energy metabolism of the visual system. Eye Brain 2, 99–116. [PubMed: 23226947]

Wu M-Y, Yiang G-T, Liao W-T, Tsai AP-Y, Cheng Y-L, Cheng P-W, Li C-Y, Li C-J, 2018. Current Mechanistic Concepts in Ischemia and Reperfusion Injury. CPB 46, 1650–1667.

Wurm A, landiev I, Uhlmann S, Wiedemann P, Reichenbach A, Bringmann A, Pannicke T, 2011. Effects of ischemia-reperfusion on physiological properties of Muller glial cells in the porcine retina. Invest Ophthalmol Vis Sci 52, 3360–3367. [PubMed: 21345997]

Xu HZ, Le YZ, 2011. Significance of outer blood-retina barrier breakdown in diabetes and ischemia. Invest Ophthalmol Vis Sci 52, 2160–2164. [PubMed: 21178141]

Yamamoto H, Schmidt-Kastner R, Hamasaki DI, Yamamoto H, Parel J-M, 2006. Complex neurodegeneration in retina following moderate ischemia induced by bilateral common carotid artery occlusion in Wistar rats. Experimental Eye Research 82, 767–779. [PubMed: 16359664]

Yamori Y, Horie R, Handa H, Sato M, Fukase M, 1976. Pathogenetic similarity of strokes in stroke-prone spontaneously hypertensive rats and humans. Stroke 7, 46–53. [PubMed: 1258104]

Zhang Y, Fortune B, Atchaneeyasakul LO, McFarland T, Mose K, Wallace P, Main J, Wilson D, Appukuttan B, Stout JT, 2008. Natural history and histology in a rat model of laser-induced photothrombotic retinal vein occlusion. Curr Eye Res 33, 365–376. [PubMed: 18398711]

Zheng W, Matei N, Pang J, Luo X, Song Z, Tang J, Zhang JH, 2019. Delayed recanalization at 3 days after permanent MCAO attenuates neuronal apoptosis through FGF21/FGFR1/PI3K/Caspase-3 pathway in rats. Exp Neurol 320, 113007. [PubMed: 31295445]

Highlights

- Reduction in oxygen metabolism is related to visual dysfunction, retinal thinning, gliosis and apoptosis markers after ischemia/reperfusion injury
- Impairment in retinal oxygen metabolism shortly after ischemia/reperfusion predicted visual function and retinal thickness outcomes

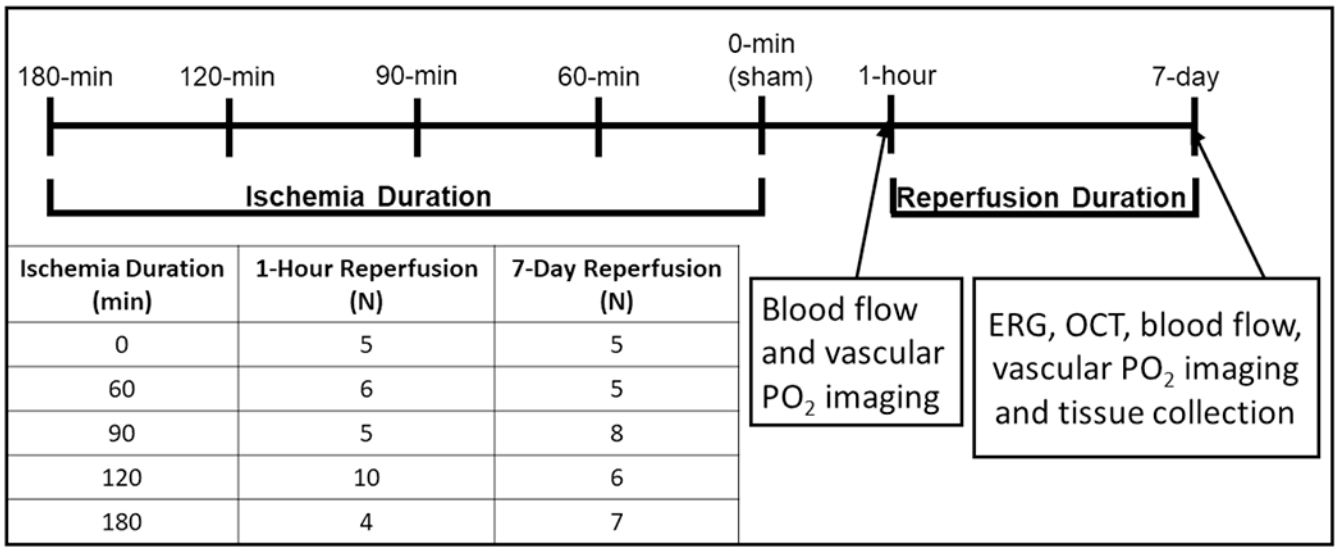

Ischemia Duration (min)	1-Hour Reperfusion (N)	7-Day Reperfusion (N)
0	5	5
60	6	5
90	5	8
120	10	6
180	4	7

Figure 1. Study design and groups

Diagram of the sequence of various quantities assessed after ophthalmic vessel occlusion (OVO). Rats underwent unilateral OVO or sham surgery. Animals were divided into 5 ischemia duration groups (0 [sham], 60, 90, 120 and 180 minutes) and 2 reperfusion duration (1 hour, 7 days) groups. ERG: Electroretinography, OCT: spectral-domain optical coherence tomography, PO_2: vascular oxygen tension.

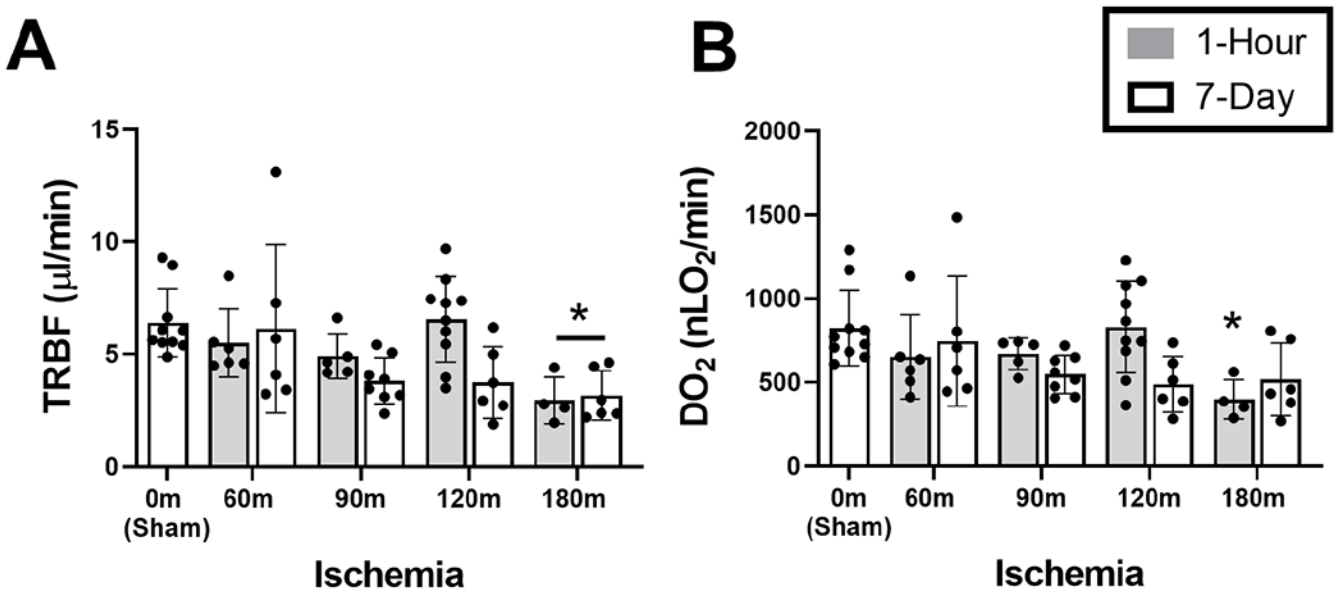

Figure 2. Retinal blood flow and oxygen delivery following ophthalmic vessel occlusion

Measurements of retinal oxygen metrics stratified by ischemia duration of 0 (sham), 60, 90, 120 and 180 minutes, and reperfusion durations of 1 hour or 7 days. (A) Total retinal blood flow (TRBF) and (B) oxygen delivery (DO_2). The data are presented as mean ± SD. Different of animals were evaluated in each group. * denotes significant difference compared to the sham group.

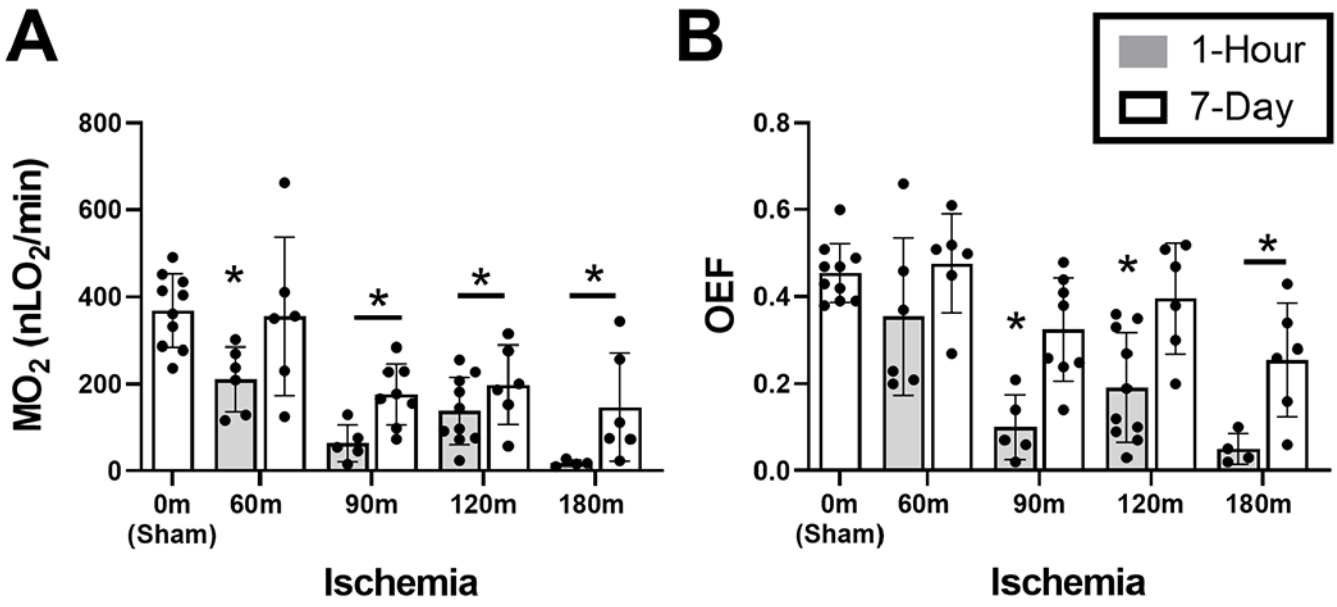

Figure 3. Retinal oxygen metabolism and extraction fraction following ophthalmic vessel occlusion

Measurements of retinal oxygen metrics stratified by ischemia duration of 0 (sham), 60, 90, 120 and 180 minutes, and reperfusion durations of 1 hour or 7 days. (A) Oxygen metabolism (MO_2) and (B) Oxygen extraction fraction (OEF). The data are presented as mean ± SD. Different of animals were evaluated in each group. * denotes significant difference compared to the sham group.

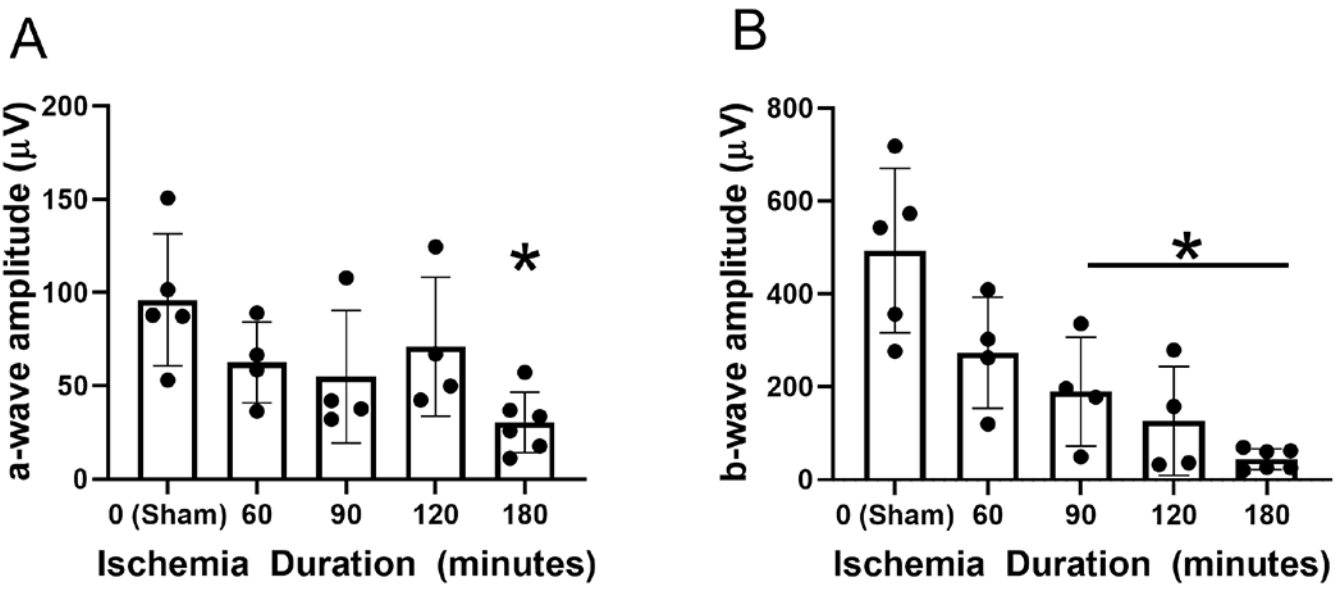

Figure 4. Retinal electrophysiological function following ophthalmic vessel occlusion

Measurements of (A) a- and (B) b-wave amplitude after 7 days of reperfusion, stratified by duration of ischemia. The data are presented as mean ± SD. * denotes significant difference compared to the sham group.

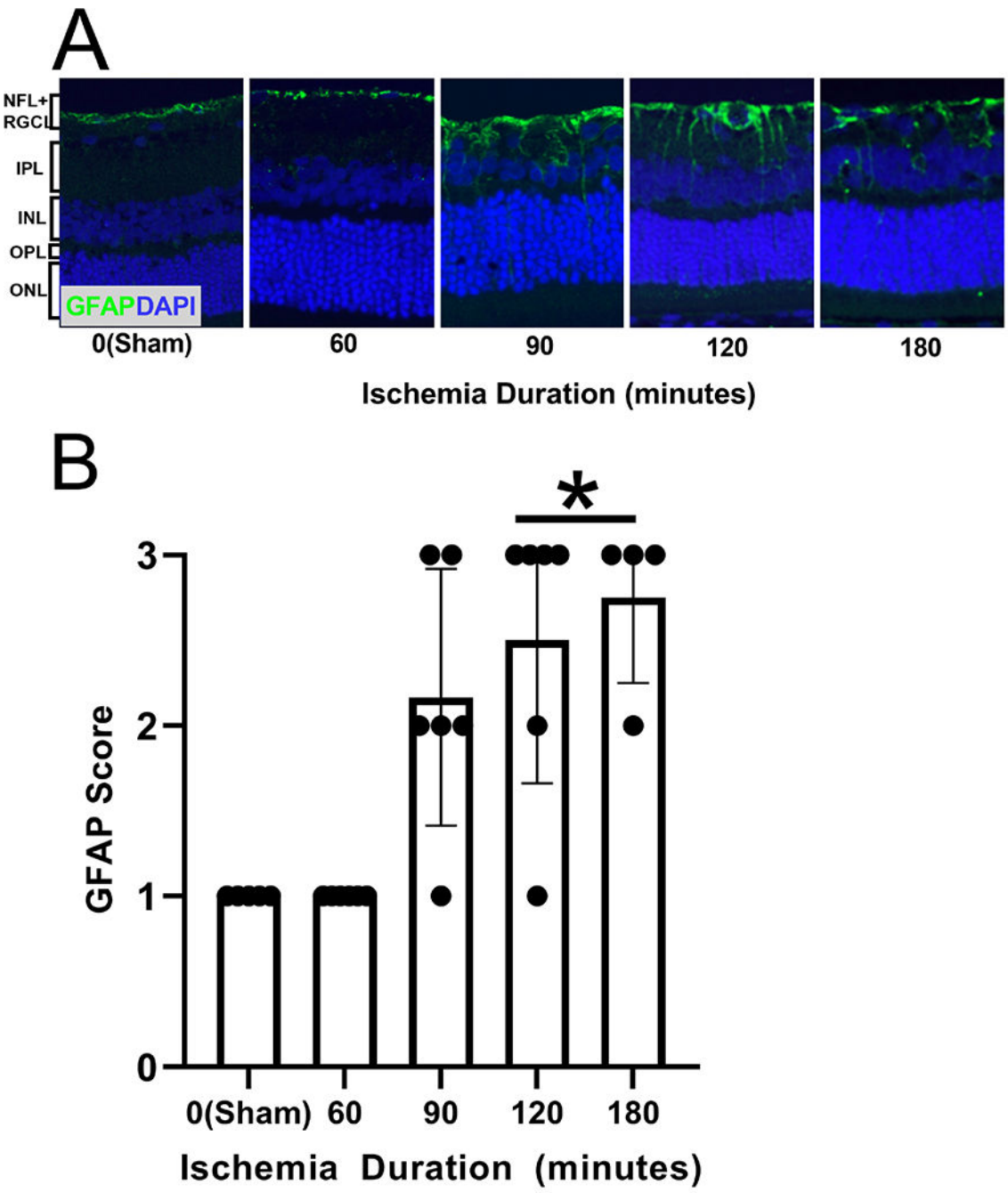

Figure 5. Retinal gliosis following ophthalmic vessel occlusion

(A) Glial fibrillary acidic protein (GFAP) in representative retinal sections of 0-minute (sham), 60-minute, 90-minute, 120-minute, and 180-minute ischemia duration groups. Active gliosis is depicted as the green color, and cell nuclei are depicted as the blue color (DAPI). (B) GFAP score (gliosis scoring system ranging from 0-3) measured after 7 days of reperfusion, stratified by duration of ischemia. The data are presented as mean ± SD. NFL: nerve fiber layer, RGCL: retinal ganglion cell layer, IPL: inner plexiform layer, INL: inner

nuclear layer, OPL: outer plexiform layer, ONL outer nuclear layer. * denotes significant difference compared to the sham group.

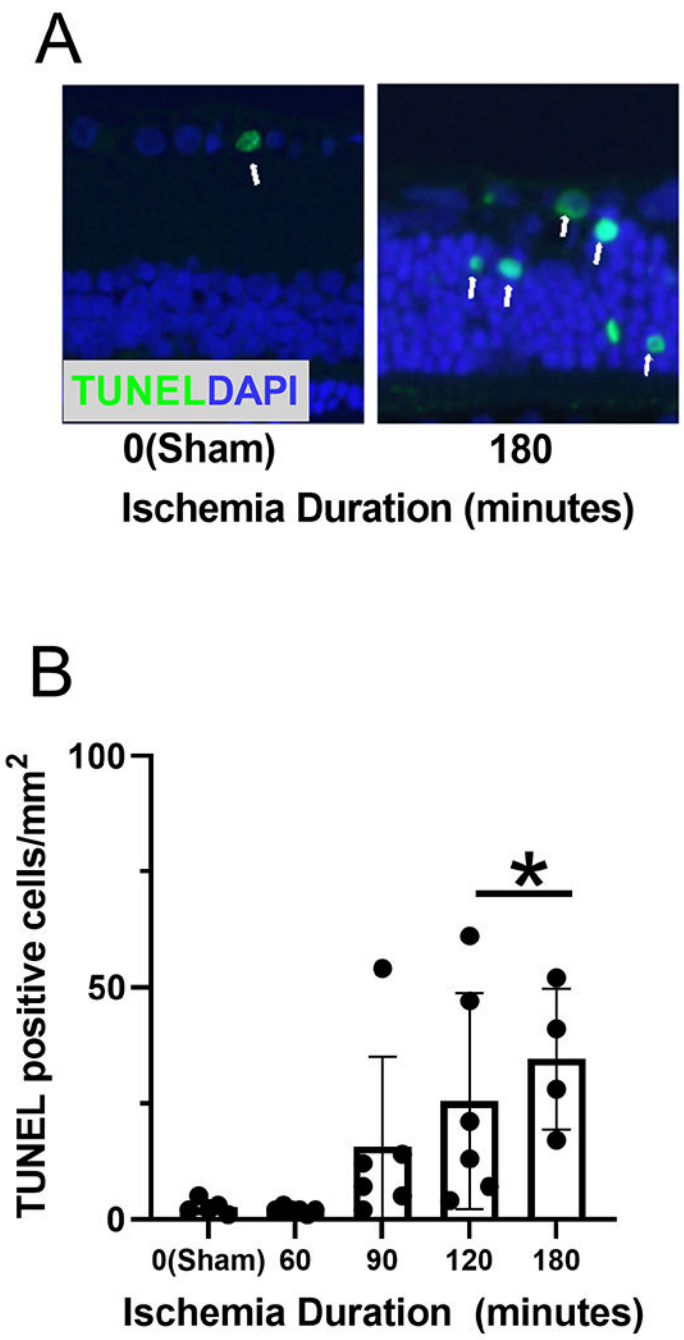

Figure 6. Retinal apoptotic cells following ophthalmic vessel occlusion

(A) TUNEL staining, depicted as the green color, colocalized with cell nuclei, presented as blue color (DAPI) in representative retinal sections. The white arrows indicate co-expression in the same cell. (B) The number of TUNEL-positive cells measured after 7 days of reperfusion, stratified by duration of ischemia. The data are presented as mean ± SD. * denotes significant difference compared to the sham group.

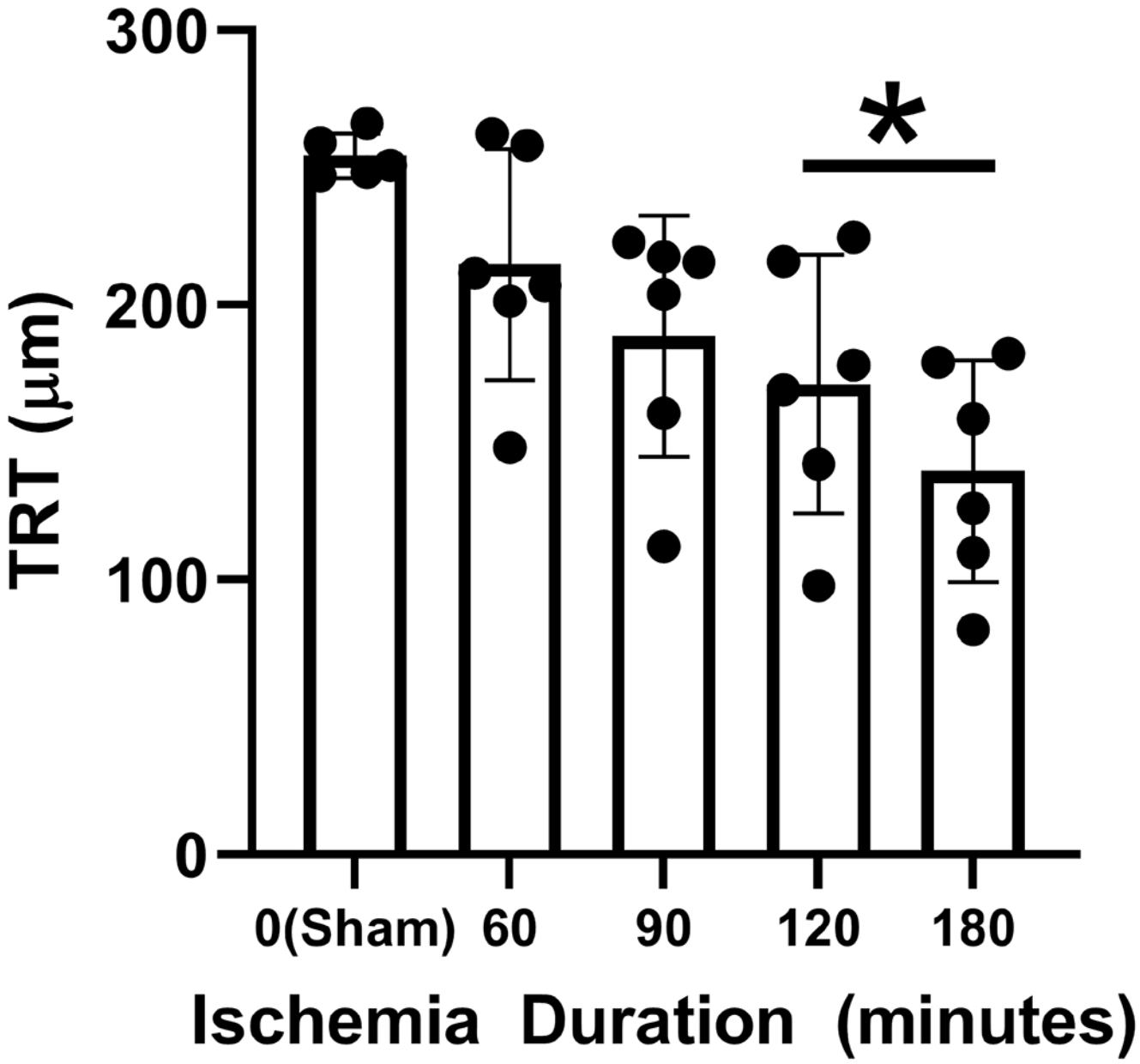

Figure 7. Retinal thickness following ophthalmic vessel occlusion

Total retina thickness (TRT) measured after 7 days of reperfusion, stratified by duration of ischemia. The data are presented as mean ± SD. * denotes significant difference compared to the sham group.

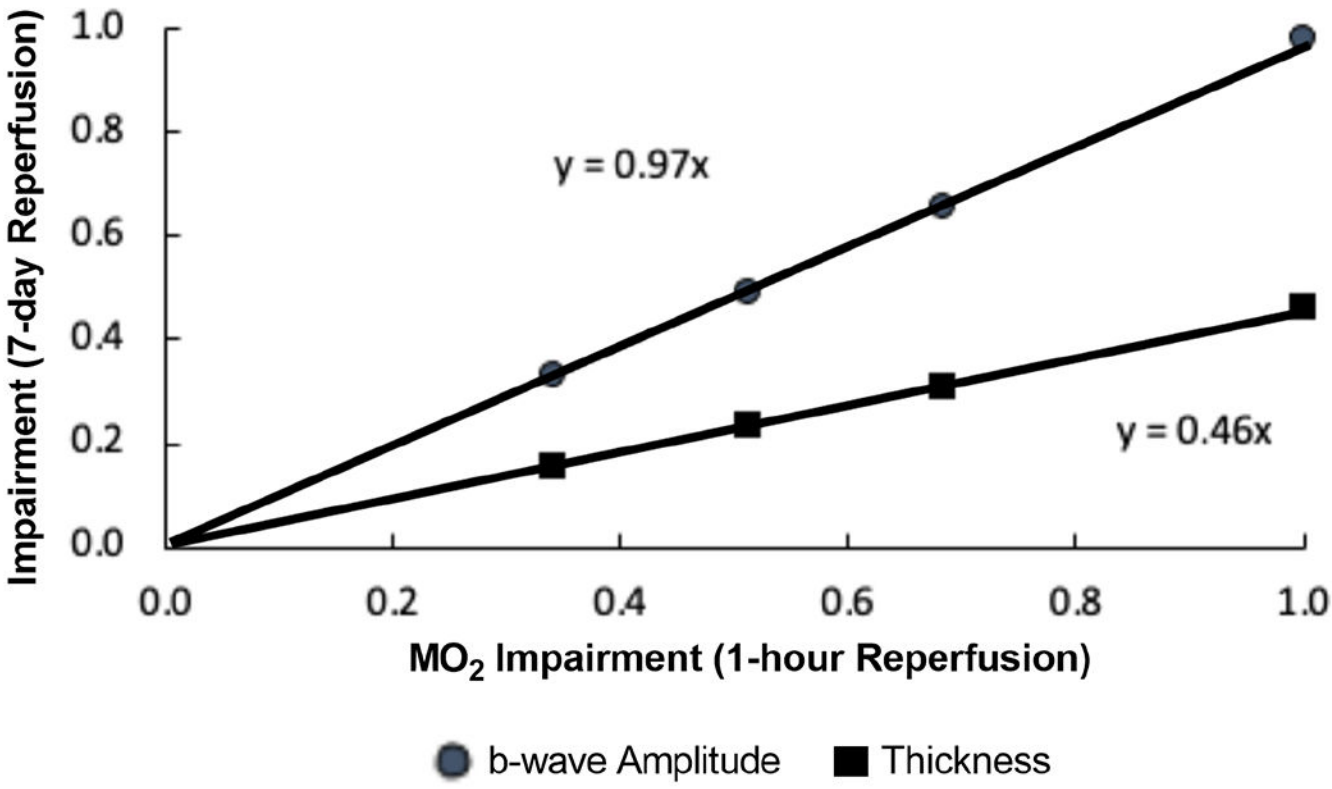

Figure 8. Relationships of MO_2, b-wave amplitude and total retinal thickness impairment indices following ophthalmic vessel occlusion

Impairment indices of b-wave amplitude and total retinal thickness (TRT) after 7-days of reperfusion are plotted as a function of MO_2 impairment index after 1-hour reperfusion.

Table 1:

Linear Regression of Variables with Ischemia Duration: y = m * (ischemia duration) + b

Variable (y)	Reperfusion Duration	N	m	b	r	P-Value
MO_2, nLO_2/min	1-hour	35	−1.97	346	0.82	<0.0001
ERG b-wave amp, μV	7-days	23	−2.46	452	0.82	<0.0001
TRT, μm	7-days	29	−0.64	252	0.72	<0.0001

MO_2: inner retinal oxygen metabolism, ERG b-wave amp: electroretinograph b-wave amplitude, TRT: total retinal thickness.